ENVIRONMENTAL RESEARCH
CLIMATE

PURPOSE-LED PUBLISHING™

PAPER • OPEN ACCESS

Kicking the can down the road: understanding the effects of delaying the deployment of stratospheric aerosol injection

To cite this article: Ezra Brody *et al* 2024 *Environ. Res.: Climate* **3** 035011

ENVIRONMENTAL RESEARCH
CLIMATE

PAPER

Kicking the can down the road: understanding the effects of delaying the deployment of stratospheric aerosol injection

Ezra Brody[1,*], **Daniele Visioni**[2], **Ewa M Bednarz**[1,3,4], **Ben Kravitz**[5,6], **Douglas G MacMartin**[1], **Jadwiga H Richter**[7] and **Mari R Tye**[7,8]

[1] Department of Mechanical and Aerospace Engineering, Cornell University, Ithaca, NY, United States of America
[2] Department of Earth and Atmospheric Sciences, Cornell University, Ithaca, NY, United States of America
[3] Cooperative Institute for Research in Environmental Sciences (CIRES), University of Colorado, Boulder, Boulder, CO, United States of America
[4] NOAA Chemical Sciences Laboratory, Boulder, CO, United States of America
[5] Department of Earth and Atmospheric Sciences, Indiana University, Bloomington, IN, United States of America
[6] Atmospheric Sciences and Global Change Division, Pacific Northwest National Laboratory, Richland, WA, United States of America
[7] National Center for Atmospheric Research, Boulder, CO, United States of America
[8] Whiting School of Civil Engineering, Johns Hopkins University, Baltimore, MD, United States of America
[*] Author to whom any correspondence should be addressed.

E-mail: eb637@cornell.edu

Keywords: climate change, solar radiation modification, stratospheric aerosol injection

Supplementary material for this article is available online

OPEN ACCESS

RECEIVED
8 February 2024

REVISED
28 April 2024

ACCEPTED FOR PUBLICATION
4 June 2024

PUBLISHED
1 July 2024

Abstract

Climate change is a prevalent threat, and it is unlikely that current mitigation efforts will be enough to avoid unwanted impacts. One potential option to reduce climate change impacts is the use of stratospheric aerosol injection (SAI). Even if SAI is ultimately deployed, it might be initiated only after some temperature target is exceeded. The consequences of such a delay are assessed herein. This study compares two cases, with the same target global mean temperature of ∼1.5° C above preindustrial, but start dates of 2035 or a 'delayed' start in 2045. We make use of simulations in the Community Earth System Model version 2 with the Whole Atmosphere Coupled Chemistry Model version 6 (CESM2-WACCM6), using SAI under the SSP2-4.5 emissions pathway. We find that delaying the start of deployment (relative to the target temperature) necessitates lower net radiative forcing (−30%) and thus larger sulfur dioxide injection rates (+20%), even after surface temperatures converge, to compensate for the extra energy absorbed by the Earth system. Southern hemisphere ozone is higher from 2035 to 2050 in the delayed start scenario, but converges to the same value later in the century. However, many of the surface climate differences between the 2035 and 2045 start simulations appear to be small during the 10–25 years following the delayed SAI start, although longer simulations would be needed to assess any longer-term impacts in this model. In addition, irreversibilities and tipping points that might be triggered during the period of increased warming may not be adequately represented in the model but could change this conclusion in the real world.

1. Introduction

Increased concentrations of carbon dioxide and other greenhouse gasses (GHGs) have been causing global mean temperatures to rise. If left uncurtailed, this could lead to catastrophic outcomes to ecosystems and human lives throughout the world. Efforts are being made to decrease carbon dioxide emissions, but there are several technological and societal barriers that limit progress in this regard. These barriers make it unlikely that the world will stay beneath the 1.5-degree-above-preindustrial temperature target set by the Paris Agreement (IPCC 2018, Jewell and Cherp 2019, Gambhir *et al* 2023). Stratospheric aerosol injection (SAI) has been gaining attention as a potential method to avoid catastrophic effects of climate change while efforts are made to decrease greenhouse gas concentrations. SAI would involve lofting aerosols—typically

sulfate—or their precursors into the lower stratosphere. This would reflect a small amount of incoming solar radiation back to space, cooling the planet as a result (UNEP 2023).

There is a vast array of potential real-world scenarios in which SAI deployment could play out, making analysis of possible outcomes difficult (MacMartin *et al* 2022). These scenarios are defined by a number of variables, including the underlying GHG emission scenario (e.g. Tilmes *et al* 2020), the latitudes and strategy used for injection (Zhang *et al* 2024), the start date of a potential SAI deployment, and a desired level of cooling or temperature target. Even with just the latter two variables, there are many permutations that could occur. For a fixed start date, one could choose different levels of desired cooling—or temperature targets—and analyze the change in outcomes. This has been studied by Visioni *et al* (2023) using the middle-of-the-road SSP2-4.5 GHG emission scenario and SAI starting in 2035. On the other hand, one could choose a single SAI temperature target and vary the start date of SAI deployment. The latter is the focus of this paper, where we consider the differences in outcomes between starting SAI deployment roughly when surface temperatures reach the target, versus delaying and using SAI to cool back down to target temperature.

We choose here a relatively short 10 year difference in the start-date of deployment, intending to explore the implications of choices policy-makers might face, with a trade-off between a nearer-term deployment to reduce climate impacts or waiting a decade to provide time for more research and more robust governance development (Visioni *et al* 2024). Our simulations are set under a background emission scenario of SSP2-4.5 for reasons explained in MacMartin *et al* (2022); however, for short-term warming this choice does not lead to large differences across other emission scenarios (Tebaldi *et al* 2021). In our simulations, the 10 year difference in start date leads to a peak warming of 0.5° C above the ultimate temperature target at the start of deployment. Other choices for the scenario are also informative; Pflüger *et al* (2024), for instance, selected a much larger 60-year delay under a higher emissions scenario (SSP5-8.5), resulting in a peak warming of just over 3° C above the ultimate temperature target at the start of deployment. This allowed them to investigate the ensuing non-linear effects such as changes in ocean dynamics and, in particular, the ability of SAI to recover a large slowdown of the AMOC, which our scenario choice would not capture. As such, these two studies are complementary, covering two quite different ends of this particular scenario dimension.

These simulations have also been used by Hueholt *et al* (2024) to study the ecological impacts of the rapid cooling associated with the delayed start case, whereas we focus more on the differences between the 2035 and 2045 start-date cases. We use the original ARISE dataset described in Richter *et al* (2022), as well as two new datasets; these extended-ARISE datasets are available to the broader research community for analysis.

Understanding the effects of waiting longer to start deployment is important for policy-makers. SAI research is a young field, and there are still many important knowledge gaps (e.g. NASEM 2021) that scientists are working to address. Additionally, it may take considerable time to develop the capability to deploy SAI as it would require novel aircraft (Smith and Wagner 2018). Perhaps most importantly, the institutional capacity to make a decision on deployment as well as oversee its implementation does not yet exist. However, the downsides of waiting longer might be significant, so it is important to factor this into a decision on whether or not to deploy, or start developing the capability to deploy, at any given time.

In this study we seek to answer two broad questions: (1) Is it possible to achieve the same final climate state with a delayed deployment as with an earlier deployment? and (2) How significant are the differences in the climate damages between the two scenarios? One reason why the same climate state may not be achieved in a delayed start case is the existence of irreversible elements in the climate system, commonly referred to as tipping points. These are changes to the state of the climate system that, once triggered, cannot be reversed by simply reversing the forcing mechanism (Armstrong Mckay *et al* 2022). Such events include shifting to a different regime of the Atlantic Meridional Overturning Circulation (AMOC) (Ditlevsen and Ditlevsen 2023), ice sheet mass loss, or a reduction in the productivity in the Amazon forest (Amazon Dieback). Knowing whether delaying the start of SAI deployment could result in one of these tipping elements being triggered would be an important factor to consider when making a decision about whether to deploy at any given time. It is, however, unclear exactly how effective climate intervention methods are in preventing such tipping elements, as their associated mechanisms have varying response times (Futerman *et al* 2023). It is also worth acknowledging that some authors (e.g. Markusson *et al* 2013, Horton 2015, Patterson *et al* 2021) have raised concerns with an emergency framing around tipping points; nonetheless, a deployment of SAI has the potential to reduce the risks of crossing future tipping points.

Delayed deployment will also lead to higher injection rates being needed even for the same ultimate temperature target, as sufficient aerosols would be needed to manage the increased energy accumulated in the Earth system during the delay. This increases cost. But more importantly, this would exacerbate the physical and chemical effects related to increased sulfate load in the atmosphere. These could include stratospheric heating and the resulting modulation of stratospheric circulation (e.g. Simpson *et al* 2019, Bednarz *et al* 2023a), weakening of the Hadley cell (Cheng *et al* 2022), modulation of the extratropical modes of variability like Northern and Southern Annular Modes (Banerjee *et al* 2020, 2021, Bednarz *et al* 2022),

ozone depletion (Tilmes *et al* 2022), changes in the hydrological cycle (Simpson *et al* 2019, Tye *et al* 2022, Tew *et al* 2023), and acid rain impacts (Visioni *et al* 2020). Furthermore, the relationship between injection rate and cooling is known to be nonlinear (Visioni *et al* 2023), with diminishing returns for increased injection rates. This will further increase the needed injection rate from a delayed start. It is also important to consider not just whether the climate can eventually be returned to the same state, but the amount of time and the SO_2 injection rates that are needed to do so.

One potential benefit of delaying SAI deployment is the recovery of ozone due to the decrease in halogens in the stratosphere. SAI exacerbates the chemical ozone depleting effects of halogens as the aerosols provide active surfaces on which heterogeneous reactions can convert halogens from inactive reservoir forms (e.g. HCl, $ClONO_2$) into active, ozone-destroying forms (e.g. Cl_2, ClO) (Haywood *et al* 2022). Stratospheric halogen concentrations have been decreasing since the 1990s and are projected to continue to decrease for the next century as a result of the phase-out of the long-term ozone depleting substances introduced by the 1987 Montreal Protocol and its subsequent amendments and adjustments. It follows that waiting longer to start deploying SAI could minimize the negative impact on the ozone layer by this mechanism. However, as stated earlier, a delayed start will likely require greater injection rates and thus a greater sulfate burden, which would exacerbate southern hemispheric ozone depletion. The tradeoff between these factors is explored in this study.

This study primarily focuses on the energy imbalance, surface climate, ozone, and tipping point changes resulting from the delayed start.

2. Methodology

2.1. Model description

All simulations were run using the Community Earth System Model, version 2 (CESM2), using the Whole Atmosphere Community Climate Model, version 6 (WACCM6) for the atmosphere model. The configuration has a horizontal resolution of 1.25° longitude by 0.9° latitude. It has 70 vertical layers, with a model top at 4.5×10^{-6} hPa (∼140 km). This high top is important for resolving the stratospheric dynamics that transport the aerosols in SAI. WACCM6 also includes interactive tropospheric-stratospheric-mesospheric-lower-thermospheric chemistry, prognostic aerosols using the Modal Aerosol Model version 4, as well as an interactive sulfur cycle. This allows for representation of SO_2 oxidation and subsequent nucleation and coagulation into sulfate aerosols, as well as aerosol transport. These mechanisms are a core component of SAI, so accurate representation of these processes is important for these simulations. This model has been shown to capture these processes reasonably well (Davis *et al* 2023, Tilmes *et al* 2023). Of note, this model has a higher-than-average climate sensitivity, and predicts a stronger AMOC decline than most. (Weijer *et al* 2020). A more detailed description of CESM2(WACCM6) can be found in Danabasoglu *et al* (2020).

2.2. Reference simulations

The reference simulation used in this study is the Shared Socioeconomic Pathway scenario SSP2-4.5, which is the middle-of-the-road emissions scenario that is roughly consistent with current global climate policy (Parson *et al* 2007, Parson 2008). A 5-member ensemble of this scenario was simulated with CESM2(WACCM6) as part of the CMIP6 project for the years 2015–2100. An additional shorter 5-member ensemble, covering years 2015–2070, was produced as part of the Assessing Responses and Impacts of Solar climate intervention on the Earth system with Stratospheric Aerosols (ARISE-SAI) simulations (Richter *et al* 2022). ARISE-SAI sets out a simulation protocol, following the guidance scenario outlined in MacMartin *et al* (2022), that can be replicated by other simulation centers (e.g. Henry *et al* 2023). ARISE-SAI-1.5 was the first set of simulations, and designed to maintain a global mean temperature ∼1.5° C above preindustrial levels. The simulation protocol recommends a minimum simulation ensemble size of three members, an initial spin-up period of 10 years following deployment and 20 further years of quasi-equilibrium simulation. The nomenclature indicates the nature of the climate intervention, for instance SAI, and the global mean temperature target. In addition to ARISE-SAI-1.5, two further ensembles using CESM2(WACCM) are available for community analysis: ∼1.5° C delayed start (ARISE-SAI-DELAY) and ∼1.0° C (ARISE-SAI-1.0), described below.

2.3. Climate intervention simulations

There are three SAI scenarios examined in this study with CESM2(WACCM6). In all three scenarios sulfate aerosol precursor, namely sulfur dioxide (SO_2) gas, is injected into the lower stratosphere with the aim of reducing surface temperatures. For all three scenarios, a ten-member ensemble of simulations was carried out and the simulations use the same non-SAI forcings from the SSP2-4.5 scenario. The differences in the SAI

Table 1. Controller targets for the three scenarios. The first 10 years of the 1.37° 2045 and 1.0° 2035 scenarios gradually ramp down to these targets.

	T_0	T_1	T_2
1.5°, 2035	288.64 K	0.8767 K	−0.589 K
1.37°, 2045	288.51 K	0.880 K	−0.587 K
1.0°, 2035	288.14 K	0.849 K	−0.590 K

scenarios are in the temperature targets, as explained below, and the start year of SAI. These three scenarios are as follows: (i) a global average temperature target of 1.5° C above preindustrial with SAI starting in 2035 (already described in Richter *et al* 2022), (ii) a global average temperature target of 1.0° C above preindustrial with SAI starting in 2035, and (iii) a global average temperature target of 1.37° C above preindustrial with SAI starting in 2045. This third ensemble was originally intended to have been the same temperature target of 1.5° C as the first scenario but was unfortunately run at a slightly lower target; below we linearly interpolate between the first two sets of simulation output to generate a 2035-start dataset that has the same temperature target as this 2045-start case. For the purposes of this study, 1.5° C above preindustrial is defined as the average global-mean near-surface air temperature from 2020 to 2039 in the first ensemble member of the SSP2-4.5 simulation in CESM2(WACCM6) (see detailed explanation in Richter *et al* 2022); 2020–2039 was chosen as representative of the time period when the Earth's global mean temperature is likely to reach 1.5° C above preindustrial (MacMartin *et al* 2022). The 1.0° C target corresponds to the 2000–2019 average, and the 1.37° C target in the 2045-start run corresponds to the 2015–2035 average.

All of the simulations use the same SAI injection strategy developed in Kravitz *et al* (2017) (and used in Tilmes *et al* 2018, 2020, MacMartin *et al* 2022, Richter *et al* 2022) that employs a feedback algorithm to adjust SO_2 injection rates at four different latitudes to maintain three large-scale near-surface air temperature metrics. The four SO_2 injection locations used here are 30° S, 15° S, 15° N, and 30° N, all at 0° E, and ∼21.5 km altitude, and the three climate outcomes are the global mean temperature (T_0), the interhemispheric temperature gradient (T_1), and the equator-to-pole temperature gradient (T_2). Complete formulas and definitions for T_1 and T_2, as well as the complete control law used in these simulations, are defined in Kravitz *et al* (2017). Values for T_0, T_1, and T_2 used in the controllers for the three scenarios are listed in table 1; the target values for T1 and T2 are chosen as the average values over the reference period in the SSP2-4.5 simulation consistent with the choice of T0 target. In the 2045 simulation, the initial temperature is significantly above the ultimate target, and a smooth transition was obtained by ramping down the target linearly to those listed in the table over the first 5 years of the simulation. In the 1.0° C 2035 simulation, the target values were ramped down linearly over the first 10 years of the simulation. Injections occur at each timestep in the model; at the end of the year, the controller calculates the new injection rates for the following year.

2.4. Interpolated simulation

The goal of this study is to isolate the effect of delaying the start of SAI deployment. In order to make a direct comparison between start dates, we need an ensemble of 2035-start but 1.37° C target simulations. We obtain these simulations via interpolation: the data for this scenario is calculated by taking a linear combination of the 2035 start 1.5° C run (74%) and the 2035 start 1.0° C run (26%). While we acknowledge the limitations of this method, as the climate is a nonlinear system, we note that the responses of certain climate variables to a forcing like GHG or SAI have been shown to be reasonably linear with small changes in surface temperature (MacMartin and Kravitz 2016, IPCC 2021, Visioni *et al* 2023, Farley *et al* 2024) and as such the method constitutes a reasonable compromise in lieu of having an ensemble of 2035-start 1.37° C target simulations.

From here on out, the reference simulations with no SAI will be called 'SSP2-4.5,' the interpolated simulations with a 2035 start and 1.37° target will be called 'SAI 2035,' and the simulations with a 2045 start and 1.37° target will be called 'SAI 2045.' Figure 1(B) shows the time evolution of the global mean near-surface air temperature in these simulations. For all subsequent discussions, the reference period refers to the 1.37°-above-preindustrial target, which corresponds to the average over 2015–2035.

3. Results and discussion

The timeseries of SO_2 injection rates in the SAI 2035 and SAI 2045 scenarios are shown in figure 2, summed over the four injection latitudes. SAI 2045 requires significantly higher injection rates than the SAI 2035 scenario—approximately 20% higher in the last decade of simulation. This is the case even after the initial cooling period (figure 2(A)), indicating that even though the global mean surface air temperatures are the same, the overall climate state is not, which is consistent with Pflüger *et al* (2024). The change in radiative

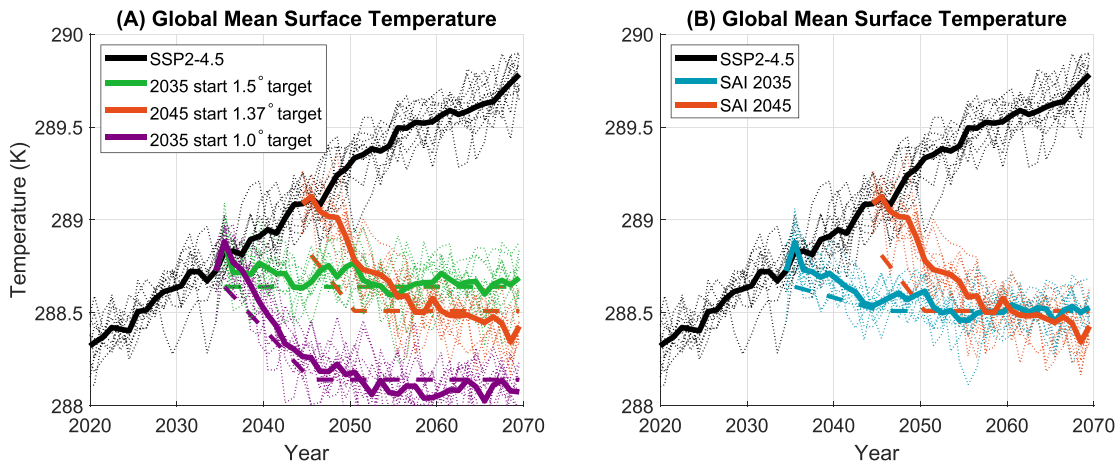

Figure 1. Global mean surface air temperature vs time. Thick solid lines represent ensemble averages. Thin dotted lines represent individual ensemble members. Thick dashed lines represent the controller targets.(A) Direct Results from the simulations. (B) The scenarios used for this study. 'SAI 2035' is a linear interpolation of '2035 start 1.5° target' and '2035 start 1.0° target' in panel A.

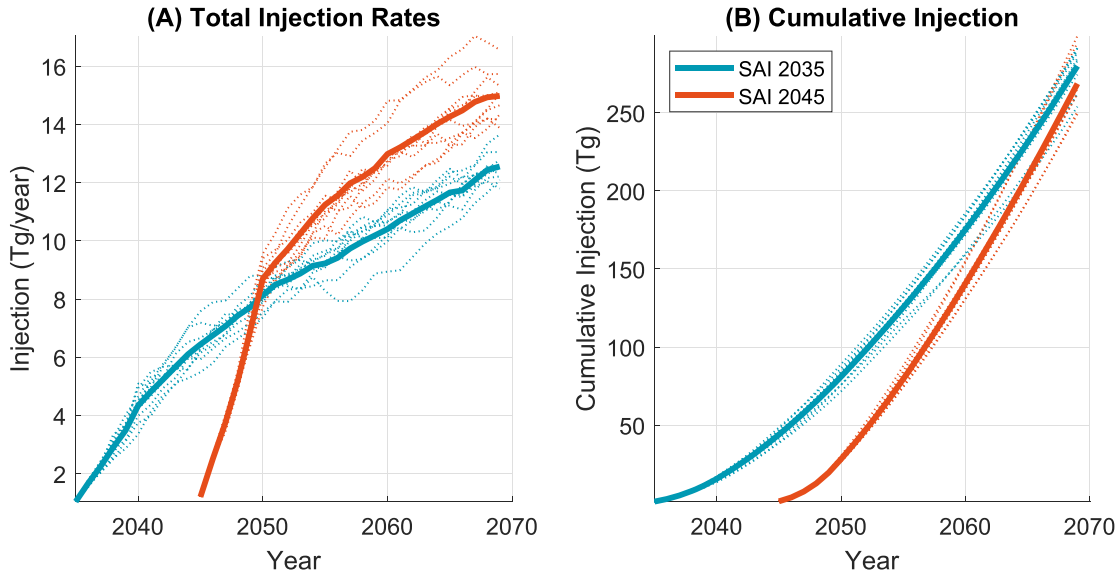

Figure 2. Left (2A)—Total SO_2 injection rates each year, summed over the four injection latitudes. Right (2B)—cumulative SO_2 injections, summed over the four injection latitudes.

forcing resulting from a change in injection rate is known to be nonlinear due to increased aerosol coagulation at higher injection rates (Visioni *et al* 2023), so the exact magnitude of the difference shown with the linear interpolation SAI 2035 scenario may be inaccurate. However, a nonlinear calculation yielded very similar results (see supplemental material). Interestingly, cumulative injections for the two scenarios are similar at the end of the simulations around 2070 (figure 2(B)), but given the known nonlinearities and limited simulation duration, it is unclear whether they would converge past 2070. This has implications for the total long-term cost of an SAI program. Given the higher long-term injection rates of SAI 2045, it would require a larger fleet of aircraft than SAI 2035. If SAI 2045 also requires a greater amount of cumulative injection in the long-term, then that will add an additional cost over SAI 2035 in the form of sulfur dioxide. Furthermore, the increased stratospheric aerosol loads under higher injection rates in SAI 2045 will lead to larger aerosol-induced stratospheric heating (figure 3), with implications for stratospheric and tropospheric circulations and, thus, regional surface climate (e.g., Bednarz *et al* 2023a, 2023b, Simpson et al 2019), as well as pose increased risks from acid rain as higher stratospheric aerosol loads are removed from the atmosphere (e.g. Visioni *et al* 2020).

In both SAI scenarios, the ensemble-average net downward radiative forcing at the top of the atmosphere is positive every year. This means that despite the global-mean surface temperature staying constant towards the end of the SAI simulations, the energy within the climate system is increasing. That is, the Earth is not in

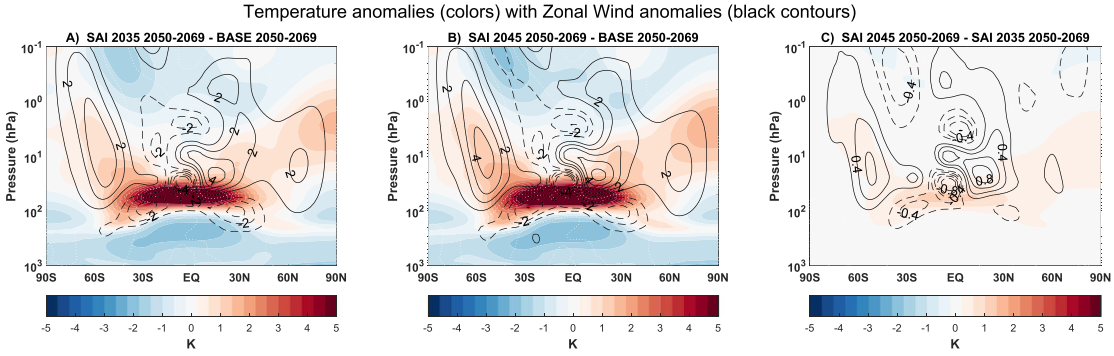

Figure 3. Difference in 2050–2069 average zonal mean temperature (colors) and zonal mean zonal winds (contours) between: (A) SAI 2035 and SSP2-4.5, (B) SAI 2045 and SSP2-4.5, and (C) SAI 2045 and SAI 2035.

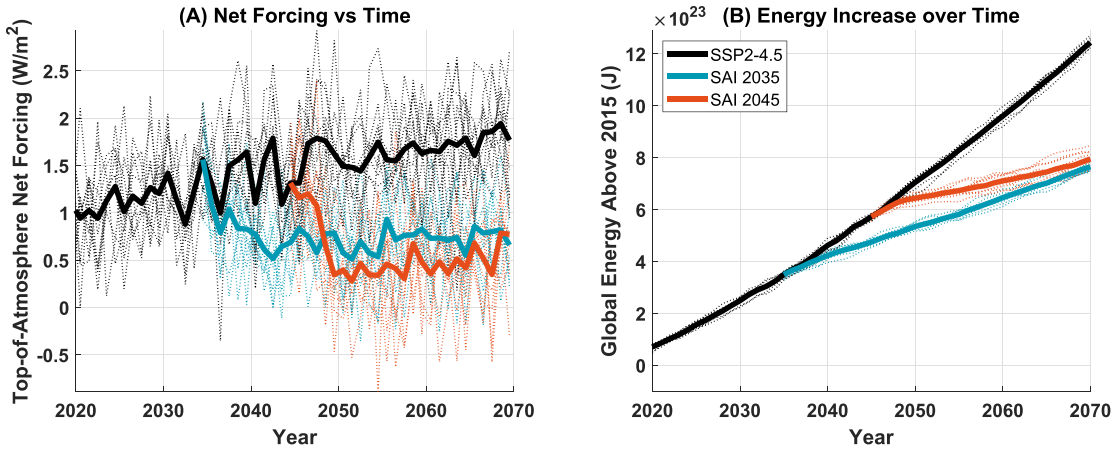

Figure 4. Left panel (A)—Total top-of-atmosphere net forcing vs time. Right panel (B)—Global energy increase above 2015 levels, calculated by integrating the left panel plot over time.

thermal equilibrium, with the deep ocean continuing to warm. Furthermore, figure 4(A) shows that after the initial transient, SAI 2045 has an approximately 30% lower net forcing than SAI 2035 due to higher sulfate aerosol loading, despite the same surface temperature. By 2070, the total energy of the climate system in the 2045 scenario is nearly equal to that of the 2035 scenario with the same temperature target.

Figure 5 shows the spatial differences in surface temperature and precipitation between the scenarios from 2055 to 2069, after global mean surface temperatures have converged. There are detectable differences in surface temperature in certain regions between SAI 2045 and SAI 2035 in annual mean. These differences are small, however, compared to the differences between either SAI scenario and SSP2-4.5. Figure S8 shows the December–January–February spatial differences; there is a slightly larger winter-warming signal over Northern Eurasia under the delayed-start case. This is likely the result of the higher injection rates and the associated stronger tropical stratospheric heating leading to a stronger high latitude response and the associated positive NAO response at the surface (Bednarz *et al* 2023a, 2023b)

Pflüger *et al* (2024) found a significant difference in the pattern of surface air temperature between their gradual-start and 70-year-delayed case that was a result of an inability of their delayed-case to restart deep-convection and recover the strength of the AMOC. Here we find no statistically significant difference in AMOC strength with our 10 year delay by the end of the simulation (figure S5), suggesting that the overall length of delay and warming during that period can affect conclusions.

For precipitation, there are very few areas that are statistically significant between SAI 2035 and SAI 2045. They are all small in area, small in magnitude, or over the ocean. Both SAI scenarios show significant differences in precipitation from SSP2-4.5. The main differences are a shift in the tropical precipitation belt and a small but consistent difference in precipitation at high latitudes.

These findings are corroborated by figure 6. Global mean precipitation increases over time in SSP2-4.5, but decreases to below the reference period level in both SAI scenarios. The two SAI scenarios have very similar amounts of precipitation over the last ∼15 years. Likewise, the ITCZ shifts southward in SSP2-4.5, but the location remains relatively steady in both SAI scenarios.

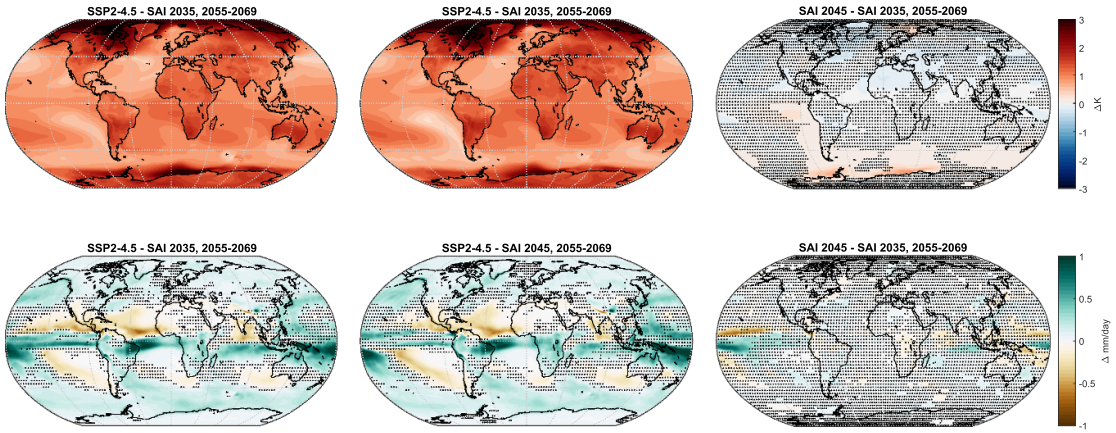

Figure 5. Average temperature difference from 2055 to 2069 between: SSP2-4.5 and SAI 2035 (top left), SSP2-4.5 and SAI 2045 (top middle), and SAI 2045 and SAI 2035 (top right). Bottom row is the same but for precipitation. Statistically insignificant areas are stippled.

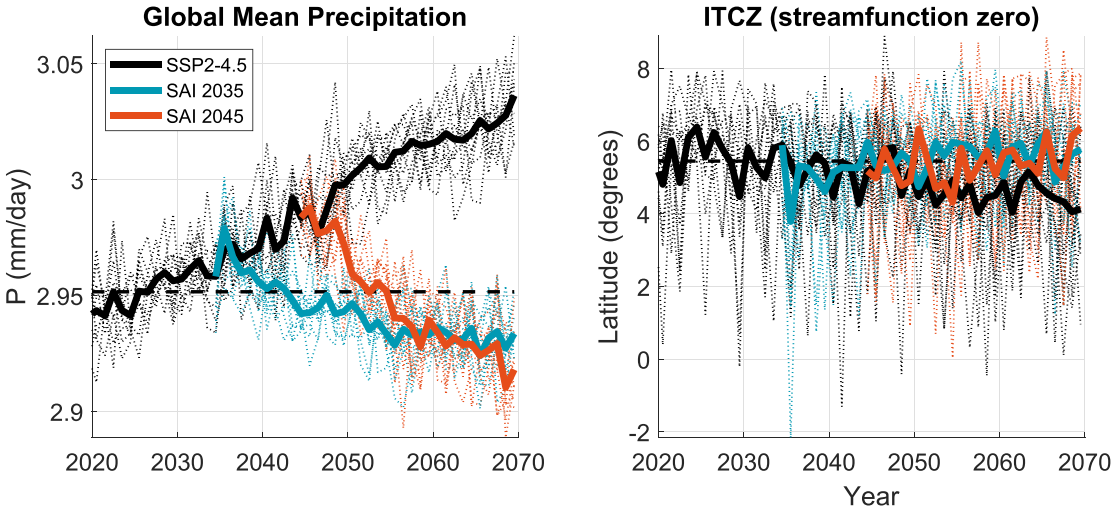

Figure 6. Global mean precipitation (left) ITCZ as the meridional streamfunction zero (Haigh *et al* 2005) (right) vs time for the three scenarios. Black dashed lines are values from the reference period (2015–2035).

Figure 7 shows the time evolution of the Arctic September sea ice (SSI) extent for the three scenarios. In general, March sea ice extent over the Arctic is not projected to change significantly over the next several decades under SSP2-4.5 in this model, and the addition of SAI does not change that significantly in any of the simulations (not shown). However, September Arctic sea ice is projected to decrease significantly over the next several decades under the SSP-2.45 scenario, and the CESM2(WACCM6) simulations suggests that SAI can reverse this decline under both SAI scenarios, indicating that at least in this model, the additional sea ice decline between 2035 and 2045 is fully reversible by a delayed-SAI. The difference in SSI extent between the 2035 and 2045 cases from 2055 to 2069 is not statistically significant at the 95% level ($p = .9109$). However, in both SAI scenarios SSI extent does not quite reach the same level as in the reference period, and this difference is statistically significant (p values of .0488 and .0251 for the 2035 start and 2045 start cases, respectively, using a t-test with ensemble members as samples).

Figure 8 shows how land carbon north of 50° N changes in the three scenarios. Total ecosystem carbon increases throughout the simulations for all scenarios as increased CO_2 and temperatures increase plant life (Lee *et al* 2023). Soil carbon increases more over time in SAI scenarios, whereas vegetation carbon increases more in SSP2-4.5. In SAI 2045, this increase in soil carbon lags behind that of SAI 2035. The plots on the bottom of figure 8 suggest that this difference is mainly a difference in permafrost. Permafrost area decreases throughout SSP2-4.5, but the rate of loss is slowed in SAI 2035. In SAI 2045, permafrost area recovers in the first 15 years or so and reaches similar levels to that of SAI 2035 by 2070. However, the soil carbon lost due to permafrost thaw cannot be recovered by simply refreezing the soil. Figure 8 (bottom right) shows that significant area at high latitudes has less carbon long-term in SAI 2045 than in SAI 2035, indicative of at least

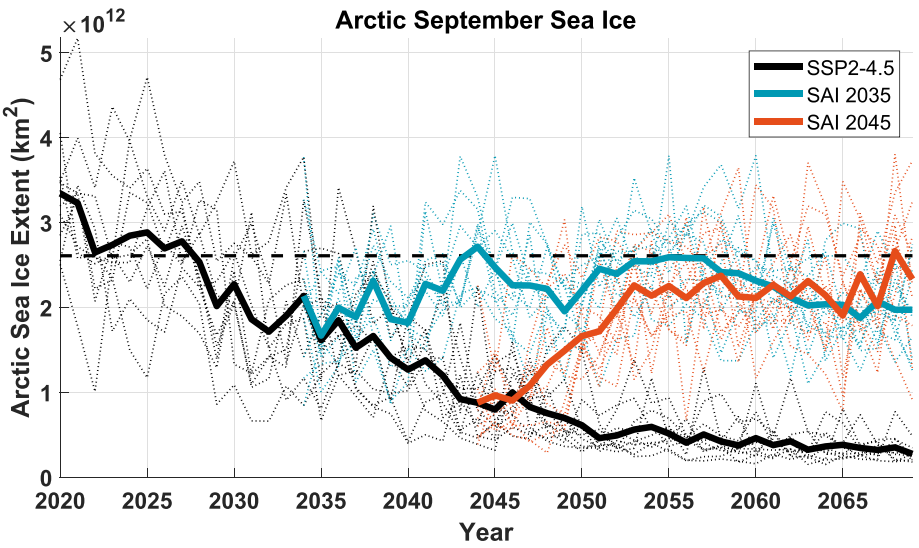

Figure 7. Plot of Arctic September sea ice vs time for the four simulations. The dashed black line represents the average value from the reference period (2015–2035).

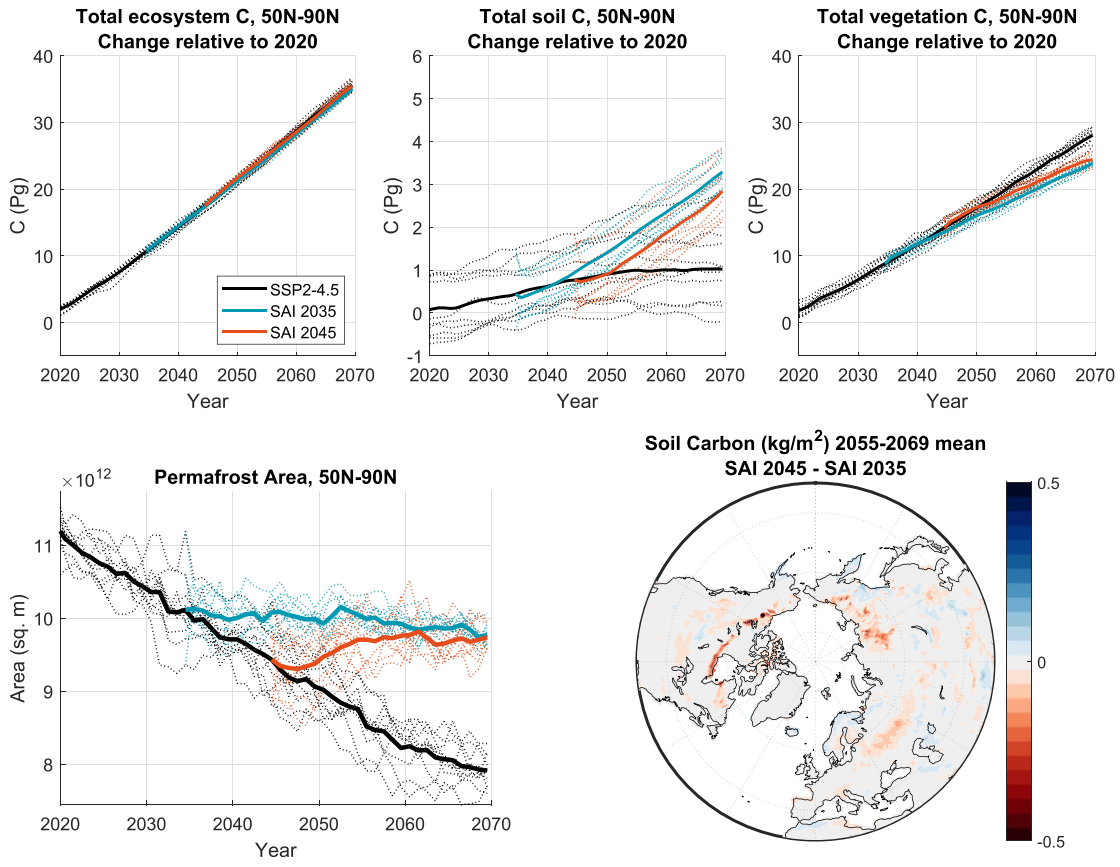

Figure 8. Time series of total land Carbon (top left), soil Carbon (top middle), vegetation Carbon (top right), and permafrost area (bottom left) north of 50° N for the three scenarios. Permafrost is defined as an area where the active layer thickness is less than 3 m year-round. Bottom right shows the spatial difference in soil carbon between SAI 2045 and SAI 2035, averaged from 2055 to 2069.

450 Tg of carbon released by permafrost thaw that is not recoverable on these time scales with the later SAI start date.

Figure 9 shows the potential temperature in parts of the ocean in contact with the Antarctic ice sheet, which are thus important in controlling ice sheet melting. The ocean temperature in the entire shelf ocean increases steadily throughout the simulation duration in SSP2-4.5. In the East Antarctic Ice Sheet (EAIS)

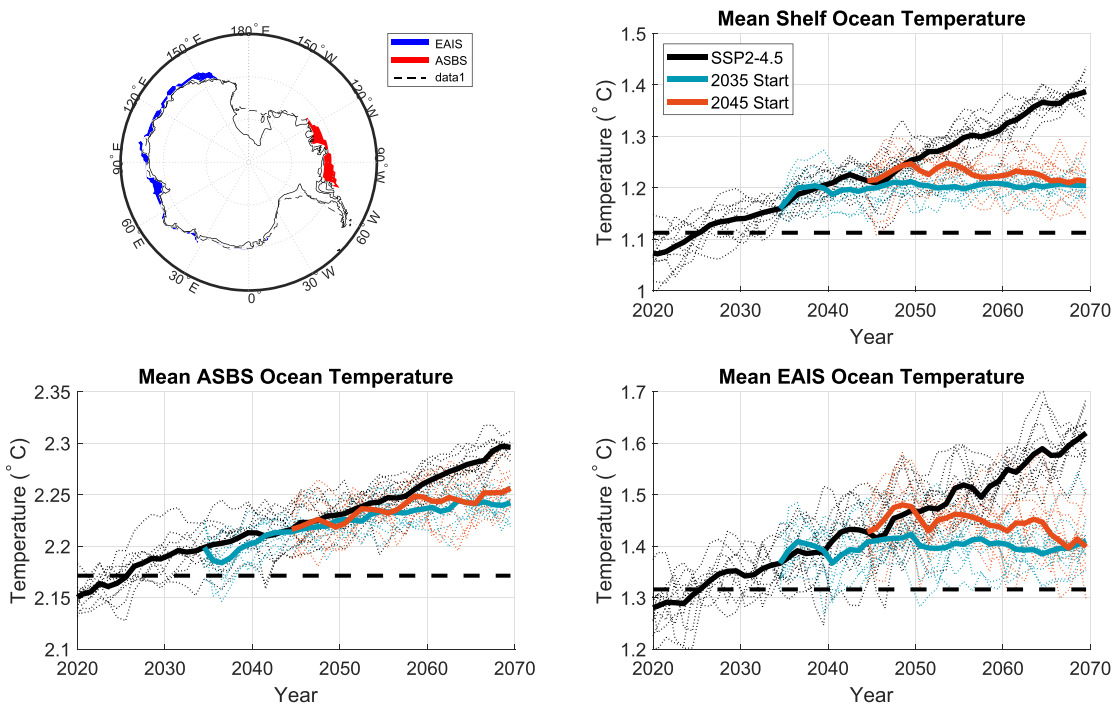

Figure 9. Top left defines the regions referenced by the other panels. The shelf ocean is defined as the area where the ocean depth is less than 1500 m, which is outlined with a dashed black line. The areas in blue and red are subregions of the shelf ocean—the East Antarctic Ice Sheet (EAIS) and Amundsen Sea Bellingshausen Sea (ASBS), respectively. The other panels show time series of mean potential temperature from 200 to 1000 m depth in the three regions. The dashed black lines represent the values from the reference period (2015–2035).

region, SAI halts this temperature increase within a few years of deployment, but in the Amundsen Sea/Bellingshausen Sea (ASBS) region, SAI slows but does not stop this increase by 2070. This arises because of the SAI-induced changes in atmospheric circulation and surface wind shear in the Antarctic region and its subsequent impacts on ocean circulation and upwelling, as detailed in Goddard *et al* (2023). In the EAIS region, SAI 2045 recovers the ocean temperature to the same level as SAI 2035 by 2070. However, this will not recover the parts of the Antarctic ice sheet that are lost as a result of heightened temperatures between 2035 and 2070. In the ASBS region, the 10 year delay in the SAI deployment has only a small effect on the shelf ocean temperature. A much larger intervention is likely required to preserve the West Antarctic Ice Sheet (Goddard *et al* 2023).

Figure 10 shows the time series of the total column ozone in various regions. The SAI-induced ozone response differs greatly with latitude. In the Antarctic during springtime, halogen-induced ozone depletion is the strongest due to the strong and cold polar vortex favoring polar stratospheric cloud formation and halogen activation. With the long-term reduction in stratospheric halogens, as well as the GHG-induced changes in stratospheric temperatures and transport, ozone is projected to increase under SSP2-4.5 over the next several decades, and this effect is strongest in the SH high latitudes (figure 10(A)).

Under SAI, Antarctic ozone levels decrease initially once SAI is started, level off around 5–10 years after the start date, and then continue to increase at roughly the same rate as ozone in the SSP2-4.5 simulation. The initial drop is due to the formation of particularly small aerosols for the few years after the beginning of the deployment, which are particularly efficient in halogen activation (Tilmes *et al* 2008).

Both SAI scenarios see a minimum Antarctic ozone level equal to that of 10 years before SAI is deployed. In SAI 2035, the minimum level of Antarctic ozone is around the 2025 level, and in SAI 2045, the minimum level of Antarctic ozone is around the 2035 level. In the long run, however, the start date does not have a noticeable effect, due to opposing impacts from lower background halogen levels but higher stratospheric sulfate loadings for SAI 2045 strategy (compared to SAI 2035). Ozone levels are set back about 20 years in both scenarios. The trend is similar for annually-averaged ozone columns in the southern hemisphere midlatitudes, partially reflecting the contribution of the Antarctic ozone following the vortex break-up in summer, but with a much smaller magnitude (figure 10(B)).

In the tropics, ozone changes due to SAI are small compared to the natural variability from the 11 year solar cycle. There appears to be a small SAI-induced increase in ozone in this region after 2055, but it is small and the effect of the start date is inconclusive.

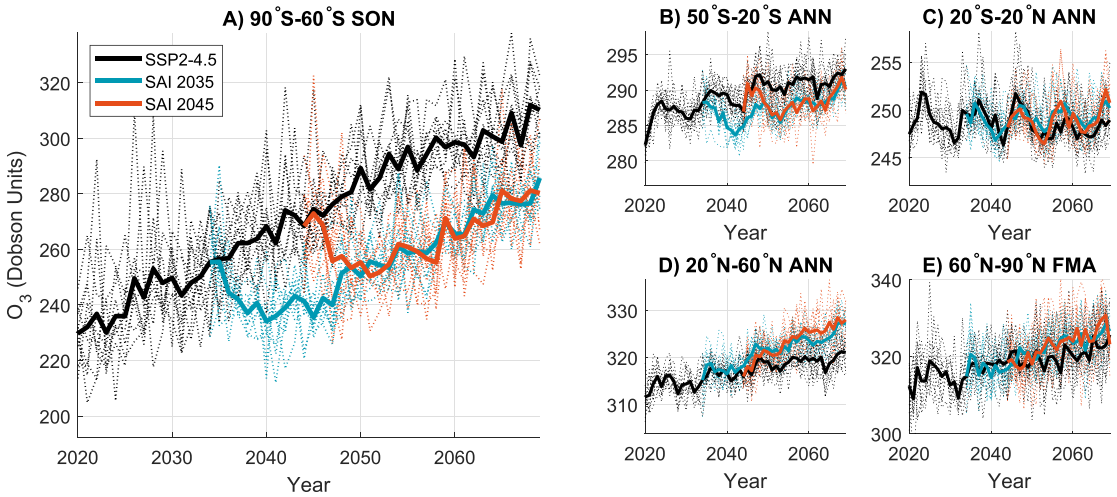

Figure 10. Total ozone column in four different regions vs time for the four simulations. From left to right, (A)—ozone column south of 60° S, averaged from September through November. (B)—ozone column from 50° S to 20° S, annually averaged. (C)—ozone column from 20° S to 20° N, annually averaged. (D)—ozone column from 20° N to 60° N, annually averaged. (E)—ozone column from 60° N to 90° N, averaged from March through May.

In the northern hemisphere, SAI increases ozone concentrations. This is a result of the corresponding acceleration of the deep branch of the Brewer–Dobson circulation, transporting more ozone poleward, as the results of aerosol-induced stratospheric heating (Bednarz *et al* 2023b). This effect accounts for the increase in total ozone columns simulated under SAI in the NH mid-latitudes compared to SSP2-4.5. Owing to the larger injection rates needed in the delayed start case to reach the same global mean surface temperatures (figure 2(A)), giving rise to larger stratospheric aerosols levels and the resulting stronger lower stratospheric heating (figure 3(C)), the acceleration of the BDC is stronger in the delayed start case, leading to larger increases in the NH total ozone columns simulated in the NH mid-latitudes. In the Arctic, while the halogen-catalyzed ozone depletion inside the polar vortex is an important driver of the Antarctic ozone, this effect is not as strong in the northern hemisphere due to generally weaker, warmer and more variable NH polar vortex. As a result, in these simulations, changing the start date of SAI does not seem to play a major role in influencing the long-term evolution of Arctic springtime ozone, although the interannual variability of the simulated springtime ozone columns is high (figure 10(E)).

4. Discussion

4.1. Conclusions from this study

The 10-member ensembles of CESM2-WACCM6 simulations under various SAI scenarios show that this strategy could be successfully used to reduce global mean temperatures to offset surface warming. The various scenarios that we considered here show that in order to reach a given temperature target, SAI could be started when that target temperature is reached, and slowly ramped up to maintain it, or it could be deployed successfully later. However, the latter strategy would require a more rapid increase in SAI to achieve the target temperature. In this latter case of delayed start of intervention, we have demonstrated here that a lower net radiative forcing (−30%) and thus a higher SO_2 injection rate (+20%) is required. This higher injection rate is needed even after global mean surface temperature converges to the target level. This would necessitate a larger SO_2 supply chain and a larger fleet of aircrafts, increasing the cost of a SAI deployment. Furthermore, the additional atmospheric sulfate load would bring with it more of the potentially undesirable physical effects associated with SAI, including stratospheric heating and acid rain.

In the model used in this study, CESM2-WACCM6, the surface air temperature, precipitation, and Arctic sea ice area are largely similar for the two start dates during the 10–25 years following the delayed SAI start, although longer simulations would be needed to assess any longer-term impacts. However, there are some climate impacts that cannot be reversed fully with SAI. Additional permafrost is lost with a delayed start, and although it can be refrozen, the carbon released into the atmosphere does not get automatically recaptured, although this may be offset by increases in ecosystem carbon. Likewise, although the Antarctic shelf ocean can be recovered to the same temperature under both scenarios, any portion of the ice sheet lost during the overshoot would not be restored. With a relatively short delay of 10 years, the AMOC in this model is recovered back to the same state even with the delay, but that is not necessarily what would happen with a

longer delay (e.g. Pflüger *et al* 2024) or in the real world. Ultimately, these risks will need to be weighed against reasons for delaying a decision to deploy, such as the increased understanding that would be gained with another decade of research. Such tradeoffs are discussed in Harding *et al* (2022).

One benefit to delaying SAI deployment is that it allows the ozone layer to recover further. The deployment strategy used in this study causes Antarctic springtime ozone levels to dip to levels from 10 years before the start of deployment before continuing to recover, so delaying SAI means the minimum ozone levels during deployment would not be as low. However, the start year of deployment does not seem to influence long-term ozone levels in the region, although the results could be sensitive to the SAI strategy chosen and the model used.

4.2. Limitations and future work

There is much more research to be done on how different SAI scenarios have different outcomes. Firstly, this study is a comparison between just two scenarios with a 10 year difference in start date. Changing this delay may yield different conclusions; for example the 60 year delay in Pflüger *et al* (2024) shows marked differences in AMOC state and an inability to restart deep convection in the North Atlantic; the difference between the 10 and 60 year delay is thus not just one of a different signal to noise ratio, but whether or not nonlinearities in the system are triggered. Studying a wider range of delays could be useful as one could start to extrapolate a general relationship between delay length and effects. Even with the same delay, changing how fast the surface climate is cooled back down to the target temperature could yield different conclusions. It is also important to evaluate a wider range of scenarios with differences aside from just the start date. Temperature targets, background emissions, and deployment inconsistencies are all important factors, and knowing how all of them affect climate outcomes is important for policy makers.

Additionally, the scenarios in this study use the same deployment strategy. The same 10 year delay with a different deployment strategy may result in different conclusions.

Even with just the simulations used in this study, there is far more analysis that could be done. For example, only four potential irreversibilities—Arctic sea ice, Arctic permafrost, AMOC, and the Antarctic ice sheet—were analyzed in this study. There are far more potential irreversibilities, such as the Greenland ice sheet and coral extinction, and output from these simulations could be used to shed light on how delaying SAI deployment could affect their associated risks. Additionally, this study only analyzed a handful of output variables in CESM2. There are far more variables, and their analysis may yield interesting conclusions that this study failed to identify.

Another important limitation is that this study uses a single climate model, CESM2 with WACCM6 as its atmospheric component. It would be valuable to conduct similar studies in other Earth system models to evaluate the robustness of conclusions.

Data availability statement

The data that support the findings of this study are openly available at the following URL/DOI: https://registry.opendata.aws/ncar-cesm2-arise/.

Acknowledgments

The authors would like to acknowledge high-performance computing support from Cheyenne (https://doi.org/10.5065/D6RX99HX) provided by NSF NCAR's Computational and Information Systems Laboratory, sponsored by the National Science Foundation, and from Amazon Web Services (AWS). Support for E Brody, D G MacMartin and D Visioni was provided in part by the Cornell Atkinson Center for a Sustainable Future and in part through Silver Lining's Safe Climate Research Initiative. Support for E M Bednarz was provided by the National Oceanic and Atmospheric Administration (NOAA) cooperative Agreement NA22OAR4320151 and the NOAA Earth's Radiative Budget (ERB) initiative. Support for B Kravitz was provided in part by the National Science Foundation through Agreement SES-1754740, NOAA's Climate Program Office, Earth's Radiation Budget (ERB) (Grant NA22OAR4310479), and the Indiana University Environmental Resilience Institute. The Pacific Northwest National Laboratory is operated for the U.S. Department of Energy by Battelle Memorial Institute under Contract DEAC05-76RL01830. The CESM project is supported primarily by the National Science Foundation. This work was in part supported by the NSF National Center for Atmospheric Research (NCAR), which is a major facility sponsored by the U.S. National Science Foundation (NSF) under Cooperative Agreement 1852977 and by SilverLining through the Safe Climate Research Initiative. The data used in this study is from the ARISE simulations, which can be found at https://registry.opendata.aws/ncar-cesm2-arise/. Data from the 2045 start simulations and 2035 start 1.0 target simulations are not available yet, but will be in the foreseeable future.

ORCID iDs

Ezra Brody https://orcid.org/0009-0003-0008-681X
Daniele Visioni https://orcid.org/0000-0002-7342-2189
Ewa M Bednarz https://orcid.org/0000-0002-7441-0497
Ben Kravitz https://orcid.org/0000-0001-6318-1150
Douglas G MacMartin https://orcid.org/0000-0003-1987-9417
Jadwiga H Richter https://orcid.org/0000-0001-7048-0781
Mari R Tye https://orcid.org/0000-0003-2491-1020

References

Armstrong Mckay D I, Staal A, Abrams J F, Winkelmann R, Sakschewski B, Loriani S, Fetzer I, Cornell S E, Rockström J and Lenton T M 2022 Exceeding 1.5° C global warming could trigger multiple climate tipping points *Science* **377** eabn7950

Banerjee A, Butler A H, Polvani L M, Robock A, Simpson I R and Sun L 2021 Robust winter warming over Eurasia under stratospheric sulfate geoengineering—the role of stratospheric dynamics *Atmos. Chem. Phys.* **21** 6985–97

Banerjee A, Fyfe J C, Polvani L M, Waugh D and Chang K-L 2020 A pause in southern hemisphere circulation trends due to the Montreal Protocol *Nature* **579** 544–8

Bednarz E M, Butler A H, Visioni D, Zhang Y, Kravitz B and MacMartin D G 2023a Injection strategy—A driver of atmospheric circulation and ozone response to stratospheric aerosol geoengineering *Atmos. Chem. Phys.* **23** 13665–84

Bednarz E M, Visioni D, Kravitz B, Jones A, Haywood J M, Richter J, MacMartin D G and Braesicke P 2023b Climate response to off-equatorial stratospheric sulfur injections in three Earth system models—part 2: stratospheric and free-tropospheric response *Atmos. Chem. Phys.* **23** 687–709

Bednarz E M, Visioni D, Richter J H, Butler A H and MacMartin D G 2022 Impact of the latitude of stratospheric aerosol injection on the southern annular mode *Geophys. Res. Lett.* **49** e2022GL100353

Cheng W *et al* 2022 Changes in Hadley circulation and intertropical convergence zone under strategic stratospheric aerosol geoengineering *npj Clim. Atmos. Sci.* **5** 32

Danabasoglu G *et al* 2020 The community earth system model version 2 (CESM2) *J. Adv. Model. Earth Syst.* **12** e2019MS001916

Davis N A *et al* 2023 Climate, variability, and climate sensitivity of "middle atmosphere" chemistry configurations of the community earth system model version 2, whole atmosphere community climate model version 6 (CESM2(WACCM6)) *J. Adv. Model. Earth Syst.* **15** e2022MS003579

Ditlevsen P and Ditlevsen S 2023 Warning of a forthcoming collapse of the Atlantic meridional overturning circulation *Nat. Commun.* **14** 1–12

Farley J, MacMartin D G, Visioni D and Kravitz B 2024 Emulating inconsistencies in stratospheric aerosol injection *Environ. Res. Clim.* (https://doi.org/10.1088/2752-5295/ad519c)

Frierson D M and Hwang Y-T 2012 Extratropical influence on ITCZ shifts in slab ocean simulations of global warming *J. Clim.* **25** 720–33

Futerman G, Adhikari M, Duffey A, Fan Y, Irvine P, Gurevitch J and Wieners C 2023 The interaction of solar radiation modification and Earth system tipping elements *Earth Syst. Dyn.* preprint (https://doi.org/10.5194/egusphere-2023-1753)

Gambhir A, Mittal S, Lamboll R D, Grant N, Bernie D, Gohar L, Hawkes A, Köberle A, Rogelj J and Lowe J A 2023 Adjusting 1.5 degree C climate change mitigation pathways in light of adverse new information *Nat. Commun.* **14** 5117

Goddard P B, Kravitz B, MacMartin D G, Visioni D, Bednarz E M and Lee W R 2023 Stratospheric aerosol injection can reduce risks to Antarctic ice loss depending on injection location and amount *J. Geophys. Res. Atmos.* **128** e2023JD039434

Haigh J D, Blackburn M and Day R 2005 The response of tropospheric circulation to perturbations in lower-stratospheric temperature *J. Clim.* **18** 3672–85

Harding A R, Belaia M and Keith D W 2022 The value of information about solar geoengineering and the two-sided cost of bias *Clim. Policy* **23** 355–65

Haywood J, Tilmes S, Keutsch F, Niemeier U, Schmidt A, Visioni D and Yu P 2022 *Stratospheric Aerosol Injection and Its Potential Effect on the Stratospheric Ozone Layer, Chapter 6 in Scientific Assessment of Ozone Depletion: 2022 GAW Report* vol 278 p 509

Henry M, Haywood J, Jones A, Dalvi M, Wells A, Visioni D, Bednarz E M, MacMartin D G, Lee W and Tye M R 2023 Comparison of UKESM1 and CESM2 simulations using the same multi-target stratospheric aerosol injection strategy *Atmos. Chem. Phys.* **23** 13369–85

Horton J B 2015 The emergency framing of solar geoengineering: time for a different approach *Anthropocene Rev.* **2** 147–51

Hueholt D, Barnes E, Hurrell J and Morrison A 2024 Climate speeds help frame relative ecological risk in future climate change and stratospheric aerosol injection scenarios *Nat. Commun.* **15** 3332

IPCC 2018 *Global Warming of 1.5° C IPCC Special Report on Impacts of Global Warming of 1.5° C above Pre-industrial Levels in Context of Strengthening Response to Climate Change, Sustainable Development, and Efforts to Eradicate Poverty* ed V Masson-Delmotte *et al* accepted

IPCC 2021 Climate change 2021: the physical science basis *Contribution of Working Group I to the Sixth Assessment Report of the Intergovernmental Panel on Climate Change* ed V P Masson-Delmotte, A Zhai, S L Pirani, C Connors, S Péan, N Berger and Y Caud

Jewell J and Cherp A 2019 On the political feasibility of climate change mitigation pathways: is it too late to keep warming below 1.5° C? *WIREs Clim. Change* **11** e621

Kravitz B, MacMartin D G, Mills M J, Richter J H, Tilmes S, Lamarque J, Tribbia J J and Vitt F 2017 First simulations of designing stratospheric sulfate aerosol geoengineering to meet multiple simultaneous climate objectives *J. Geophys. Res. Atmos.* **122**

Lee W R, MacMartin D G, Visioni D, Kravitz B, Chen Y, Moore J C, Leguy G, Lawrence D M and Bailey D A 2023 High-latitude stratospheric aerosol injection to preserve the Arctic *Earth's Future* **11**

MacMartin D G and Kravitz B 2016 Dynamic climate emulators for solar geoengineering *Atmos. Chem. Phys.* **16** 15789–99

MacMartin D G, Visioni D, Kravitz B, Richter J H, Felgenhauer T, Lee W R, Morrow D R, Parson E A and Sugiyama M 2022 Scenarios for modeling solar radiation modification *Proc. Natl Acad. Sci.* **119**

Markusson N, Ginn F, Singh Ghaleigh N and Scott V 2013 'in case of emergency press here': framing geoengineering as a response to dangerous climate change *WIREs Clim. Change* **5** 281–90

National Academies of Sciences, Engineering, and Medicine 2021 *Reflecting Sunlight: Recommendations for Solar Geoengineering Research and Research Governance* (The National Academies Press) (https://doi.org/10.17226/25762)
Parson E A 2008 Useful global-change scenarios: current issues and challenges *Environ. Res. Lett.* **3** 045016
Parson E *et al* 2007 Global-change scenarios: their development and use *(Subreport 2.1B of Synthesis and Assessment Product 2.1 by the US Climate Change Science Program and the Subcommittee onGlobal Change Research* (U.S. Global Change Research Program)
Patterson J, Wyborn C, Westman L, Brisbois M C, Milkoreit M and Jayaram D 2021 The political effects of emergency frames in sustainability *Nat. Sustain.* **4** 841–50
Pflüger D *et al* 2024 Flawed emergency intervention: slow ocean response to abrupt stratospheric aerosol injection *Geophys. Res. Lett.* **51** e2023GL106132
Richter J H, Visioni D, MacMartin D G, Bailey D A, Rosenbloom N, Dobbins B, Lee W R, Tye M and Lamarque J-F 2022 Assessing responses and impacts of solar climate intervention on the Earth system with stratospheric aerosol injection (arise-SAI): protocol and initial results from the first simulations *Geosci. Model Dev.* **15** 8221–43
Simpson I R, Tilmes S, Richter J H, Kravitz B, MacMartin D G, Mills M J, Fasullo J T and Pendergrass A G 2019 The regional hydroclimate response to stratospheric sulfate geoengineering and the role of stratospheric heating *J. Geophys. Res. Atmos.* **124** 12587–616
Smith W and Wagner G 2018 Stratospheric aerosol injection tactics and costs in the first 15 years of deployment *Environ. Res. Lett.* **13** 124001
Tebaldi C *et al* 2021 Climate model projections from the Scenario Model Intercomparison Project (ScenarioMIP) of CMIP6 *Earth Syst. Dynam.* **12** 253–93
Tew Y L, Tan M L, Liew J, Chang C K and Muhamad N 2023 A review of the effects of solar radiation management on hydrological extremes *IOP Conf. Ser.: Earth Environ. Sci.* **1238** 012030
Tilmes S *et al* 2018 CESM1(WACCM) Stratospheric Aerosol Geoengineering Large Ensemble project *Bull. Am. Meteorol. Soc.* **99** 2361–71
Tilmes S *et al* 2020 Reaching 1.5 and 2.0 °C global surface temperature targets using stratospheric aerosol geoengineering *Earth Syst. Dyn.* **11** 579–601
Tilmes S, Mills M J, Zhu Y, Bardeen C G, Vitt F, Yu P, Fillmore D, Liu X, Toon B and Deshler T 2023 Description and performance of a sectional aerosol microphysical model in the Community Earth System Model (CESM2) *Geosci. Model Dev.* **16** 6087–125
Tilmes S, Müller R and Salawitch R 2008 The sensitivity of polar ozone depletion to proposed geoengineering schemes *Science* **320** 1201–4
Tilmes S, Visioni D, Jones A, Haywood J, Séférian R, Nabat P, Boucher O, Bednarz E M and Niemeier U 2022 Stratospheric ozone response to sulfate aerosol and solar dimming climate interventions based on the G6 Geoengineering Model Intercomparison Project (geomip) simulations *Atmos. Chem. Phys.* **22** 4557–79
Tye M R, Dagon K, Molina M J, Richter J H, Visioni D, Kravitz B and Tilmes S 2022 Indices of extremes: geographic patterns of change in extremes and associated vegetation impacts under climate intervention *Earth Syst. Dyn.* **13** 1233–57
United Nations Environment Programme 2023 *One Atmosphere: An Independent Expert Review on Solar Radiation Modification Research and Deployment*
Visioni D *et al* 2024 G6-1.5K-SAI: a new geoengineering model intercomparison project (GeoMIP) experiment integrating recent advances in solar radiation modification studies *Geosci. Model Dev.* **17** 2583–96
Visioni D, MacMartin D G, Kravitz B, Bednarz E M and Goddard P B 2023 The choice of baseline period influences the assessments of the outcomes of stratospheric aerosol injection *Earth's Future* **11** e2023EF003851
Visioni D, Slessarev E, MacMartin D G, Mahowald N M, Goodale C L and Xia L 2020 What goes up must come down: impacts of deposition in a sulfate geoengineering scenario *Environ. Res. Lett.* **15** 094063
Weijer W, Cheng W, Garuba O A, Hu A and Nadiga B T 2020 CMIP6 models predict significant 21st century decline of the Atlantic meridional overturning circulation *Geophys. Res. Lett.* **47**
Zhang Y, MacMartin D G, Visioni D, Bednarz E M and Kravitz B 2024 Hemispherically symmetric strategies for stratospheric aerosol injection *Earth Syst. Dyn.* **15** 191–213